CHINESE OPTICS LETTERS

Vol. 19, No. 8 | August 2021

Spectroscopic and laser properties of Er^{3+}, Pr^{3+} co-doped $LiYF_4$ crystal

Zhengda Sun (孙政达)[1], Feifei Wang (王菲菲)[1], Haiping Xia (夏海平)[2*], Hongkun Nie (聂鸿坤)[1], Kejian Yang (杨克建)[1,3], Ruihua Wang (王瑞华)[1], Jingliang He (何京良)[1,3], and Baitao Zhang (张百涛)[1,3**]

[1] State Key Laboratory of Crystal Materials, Institute of Novel Semiconductors, Shandong University, Jinan 250100, China

[2] Key Laboratory of Crystal Materials, Ningbo University, Ningbo 315211, China

[3] Collaborative Innovation Center of Light Manipulations and Applications, Shandong Normal University, Jinan 250358, China

*Corresponding author: hpxcm@nbu.edu.cn

**Corresponding author: btzhang@sdu.edu.cn

Received December 3, 2020 | Accepted February 2, 2021 | Posted Online April 25, 2021

In this paper, the absorption and fluorescence spectra of Er^{3+}, Pr^{3+} co-doped $LiYF_4$ (Er,Pr:YLF) crystal were measured and analyzed. The Pr^{3+} co-doping was proved to effectively enhance the Er^{3+}:$^4I_{11/2} \rightarrow {}^4I_{13/2}$ mid-infrared transition at the 2.7 μm with 74.1% energy transfer efficiency from Er^{3+}:$^4I_{13/2}$ to Pr^{3+}:$^3F_4$. By using the Judd–Ofelt theory, the stimulated emission cross section was calculated to be 1.834×10^{-20} cm^2 at 2685 nm and 1.359×10^{-20} cm^2 at 2804.6 nm. Moreover, a diode-end-pumped Er,Pr:YLF laser operating at 2659 nm was realized for the first time, to the best of our knowledge. The maximum output power was determined to be 258 mW with a slope efficiency of 7.4%, and the corresponding beam quality factors $M_x^2 = 1.29$ and $M_y^2 = 1.25$. Our results suggest that Er,Pr:YLF should be a promising material for 2.7 μm laser generation.

Keywords: mid-infrared lasers; laser materials; solid-state lasers.

DOI: 10.3788/COL202119.081404

1. Introduction

Due to strong water absorption and high transmittance in the atmosphere, mid-infrared (MIR) lasers operating at the 2.7 μm wavelength band have attracted increasing attention and play a significant role in applications including medical, biological, remote sensing, free-space communication, etc.[1–3]. It can also be used as the pump source for an optical parametric oscillator (OPO) and an optical parametric amplifier (OPA) to generate even longer wavelength MIR lasers[4,5]. Er^{3+} is a well-known ion with MIR transition around 2.7 μm ($^4I_{11/2} \rightarrow {}^4I_{13/2}$). Compared with Ho^{3+} ions ($^5I_6 \rightarrow {}^5I_7$ transition around 2.9 μm), Er^{3+} ions have been extensively studied for several reasons. First, the branching ratio of Er^{3+} is twice that of Ho^{3+} for 3.0 μm laser transition. Second, Er^{3+}-doped crystals can solve the so-called "bottleneck" at 3.0 μm laser transition by high doping concentration and the efficient Auger up-conversion process, which makes it easier to realize the population inversion than Ho^{3+}-doped crystals. Third, Er^{3+}-doped crystals can be pumped by commercial 970 nm laser diodes (LDs), but Ho^{3+}-doped crystals must be pumped by the lasers around 1150 nm, which are mainly based on OPOs and Raman lasers[6–8].

However, it is worth noting that Er^{3+}-doped crystals face a serious "bottleneck" at the 2.7 μm laser transition, where the lifetime of the upper energy level ($^4I_{11/2}$) is much shorter than that of the lower energy level ($^4I_{13/2}$), resulting in the self-terminating effect[9–13]. In view of this problem, there are two mainstream solutions. One solution is to increase the doping concentration of Er^{3+} ions (atomic fraction of >30%) to increase the cross-relaxation [$^4S_{3/2}(^2H_{11/2}) \rightarrow {}^4I_{15/2}$] + ($^4I_{15/2} \rightarrow {}^4I_{13/2}$) + ($^4I_{15/2} \rightarrow {}^4I_{9/2} \rightarrow {}^4I_{11/2}$) and up-conversion ($^4I_{13/2} \rightarrow {}^4I_{15/2}$) + ($^4I_{13/2} \rightarrow {}^4I_{9/2} \rightarrow {}^4I_{11/2}$) processes to effectively decrease the lifetime of $^4I_{13/2}$. Nevertheless, on one hand, high Er^{3+} doping concentration can also lead to a large reduction in the lifetime of upper energy level $^4I_{11/2}$; on the other hand, the thermal conductivity can also be reduced at the high doping level, resulting in the serious thermal effect. The above two factors impede their applications in high-power, high-energy, and high-beam-quality MIR lasers. Another method does not require a high Er^{3+} doping concentration, in which appropriate deactivated ions are introduced to attenuate the

lifetime of the lower energy level ($^4I_{13/2}$). The Pr^{3+} ion has been proved to be an efficient deactivated ion with the energy level of $Pr^{3+}:{}^3F_4$ close to $Er^{3+}:{}^4I_{13/2}$ [13–15]. Co-doping of Er^{3+} and Pr^{3+} has been regarded as a promising alternative to quench the lower level $^4I_{13/2}$. Due to the energy transfer process between $Er^{3+}:{}^4I_{13/2}$ and $Pr^{3+}:{}^3F_4$, the terminal laser level ($Er^{3+}:{}^4I_{13/2}$) can be efficiently depopulated. Thus, the laser can operate at lower Er^{3+} ion concentrations and significantly reduce the extra heat generation caused by multiphoton relaxations. Besides, the host material also plays a great role in the MIR laser emission, which should have low phonon energy, high optical transmission at 2.7 μm, minimal H_2O absorption, and large radiative emission rate. Compared with the oxide material [846 cm^{-1} for $Y_3Al_5O_{12}$ (YAG)], the fluorides have low phonon energy [447 cm^{-1} for $LiYF_4$ (YLF)], which can suppress the non-radiative decay from the upper level $^4I_{11/2}$ to the lower level $^4I_{13/2}$, thus enhancing the MIR radiative efficiency[16,17]. Besides, negative thermal dependence of the refractive index can efficiently reduce the thermal lensing effect.

In this paper, an Er^{3+} and Pr^{3+} co-doped YLF (Er,Pr:YLF) crystal has been successfully grown by the Bridgman method. The properties of absorption and emission spectra of the Er,Pr:YLF crystal were measured and analyzed. Based on the Judd–Ofelt (J-O) theory, the emission cross section and energy transfer efficiency between $Pr^{3+}:{}^3F_4$ and $Er^{3+}:{}^4I_{13/2}$ were calculated. Furthermore, a diode-end-pumped continuous wave (CW) Er,Pr:YLF laser operating at 2659 nm was realized for the first time, to the best of our knowledge. All of these results indicate that the Er,Pr:YLF crystal has great potential for 2.7 μm laser generation.

2. Experiments and Methods

The Er,Pr:YLF crystal was grown by the Bridgman method with the initial materials of 99.99% pure LiF, YF_3, ErF_3, and PrF_3 with the molar ratio of 51.5:44.2:4:0.3[18]. The concentrations of Er^{3+} and Pr^{3+} in the Er,Pr:YLF crystal were determined to be 3.98% and 0.13%, respectively. Figure 1(a) shows the absorption spectrum with the range of 300–2400 nm measured by a U-3500 Hitachi fluorescence spectrophotometer under room temperature. The absorption peak located at 969 nm ($^4I_{15/2} \rightarrow {}^4I_{11/2}$ transition) with a full width at half-maximum (FWHM) of ~14 nm is shown in the inset of Fig. 1. Therefore, it can be pumped by the commercial ~970 nm InGaAs LD. The absorption coefficient can be calculated by the following formula:

$$\alpha = \frac{D(\lambda)}{l \times \lg e}, \tag{1}$$

where $D(\lambda)$ and l are the absorbance and the length of the crystal, respectively. The absorption coefficient at 969 nm was calculated to be ~1.86 cm^{-1}. Considering the relationship between the absorption coefficient and absorption cross section, $\sigma_{abs} = \alpha/N$, where N means the Er^{3+} ion concentration. The absorption cross section was calculated to be 0.297×10^{-20} cm^2 at the central wavelength of 969 nm.

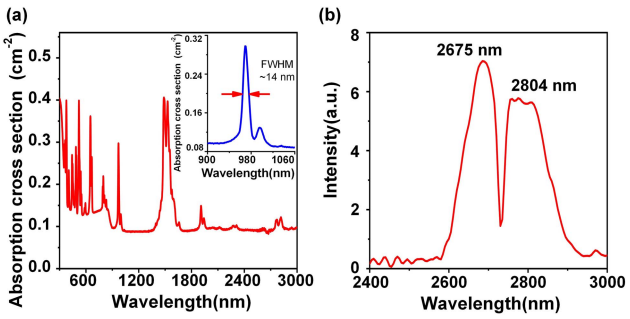

Fig. 1. Room temperature spectral properties of Er,Pr:YLF crystal: (a) absorption cross section (inset: absorption cross section within the range of 900–1060 nm); (b) fluorescence spectrum.

Figure 1(b) shows the fluorescence spectrum of Er,Pr:YLF with the spectral range of 2400–3000 nm, which was measured by Edinburgh Instruments (FLS920 and FSP920 spectrophotometers) excited by a 968 nm laser at room temperature. Two typical emission peaks located at 2685 and 2804 nm were observed. With the room temperature absorption spectra, based on the J-O theory, three typical J-O intensity parameters were calculated to be $\Omega_2 = 1.77 \times 10^{-20}$ cm^2, $\Omega_4 = 3.73 \times 10^{-20}$ cm^2, and $\Omega_6 = 4.67 \times 10^{-20}$ cm^2, respectively[19–26]. The spectroscopic quality factor $X = \Omega_4/\Omega_6$ was determined to be 0.80, which indicated that the major laser transitions were significantly strong. For the $^4I_{11/2} \rightarrow {}^4I_{13/2}$ transition, the radiative transition probability ($A_{JJ'}$), radiative lifetime of the $^4I_{13/2}$ level (τ_{rad}), and fluorescence branching ratio ($\beta_{JJ'}$) can be obtained to be 43.145 s^{-1}, 3.70 ms, and 0.121, respectively. The $^4I_{13/2}$ level lifetime was much shorter than that of the Er:YLF crystal (14.28 ms), indicating the effective deactivated function of Pr^{3+} ions.

The emission cross section (σ_{em}) of the crystal can be calculated by the Fuchtbauer–Ladenburg (F-L) equation:

$$\sigma_{em} = \frac{\lambda^5 A_{JJ'} I(\lambda)}{8\pi c n^2 \int \lambda I(\lambda) d\lambda}, \tag{2}$$

where $I(\lambda)/\int \lambda I(\lambda) d\lambda$ is the normalized line shape function of the measured emission spectrum. The stimulated emission cross section was calculated to be 1.834×10^{-20} cm^2 at 2685 nm and 1.359×10^{-20} cm^2 at 2804.6 nm, which were higher than that of Er:YLF (1.2×10^{-20} cm^2), Er:$Y_3Sc_2Ga_3O_{12}$ (Er:YSGG, 0.43×10^{-20} cm^2), and Er:YAG (0.45×10^{-20} cm^2)[26–28]. The results show that the co-doped Pr^{3+} ions effectively enhance the 2.7 μm laser emission and have enormous potentiality in realizing low-threshold and high-power laser operation.

The energy transfer efficiency (η_τ) of $Er^{3+}:{}^4I_{13/2} \rightarrow Pr^{3+}:{}^3F_4$ is an important factor to assess the effects of co-doped Pr^{3+} and can be calculated by the following equation:

$$\eta_\tau = 1 - \frac{\tau_{rad}}{\tau_{Er}}, \tag{3}$$

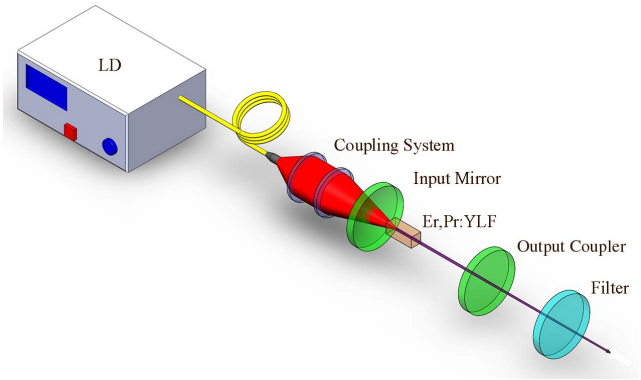

Fig. 2. Schematic setup of LD end-pumped Er,Pr:YLF laser.

where τ_{Er} is the theoretical lifetime of $^4I_{13/2}$ in Er:YLF, which was calculated to be 14.28 ms[22]. Therefore, the energy transfer efficiency was calculated to be 74.1%, indicating that co-doped deactivator Pr^{3+} ions can effectively reduce the $^4I_{13/2}$ lifetimes of Er^{3+} by resonant energy transferring.

Considering the beneficial spectral characteristics, a CW laser operation was realized. The experimental setup is shown in Fig. 2. A compact concave-plane cavity was designed with the cavity length of 14 mm. A fiber-coupled 976 nm LD with a core diameter of 200 μm and a numerical aperture of 0.22 was used as the pump source. The pump light was focused onto the crystal by a focus system with a focal length of 46.5 mm and a polarization ratio of 1:1. An uncoated *a*-cut Er,Pr:YLF with dimensions of 3 mm × 3 mm × 10 mm was wrapped with indium foil and mounted in copper block cooled by water at a temperature of 16°C. The input concave mirror with a radius of 200 mm was high-reflection (HR) coated at 2600–3050 nm and high-transmission (HT) coated at 900–1000 nm. The plane output couplers (OCs) with two different transmissions of 1% and 3% at 2600–3050 nm were used.

3. Results and Discussion

Figure 3(a) shows the laser output power as a function of the absorbed pump power with different transmissions of OCs. The maximum output power of 258 mW was obtained with a

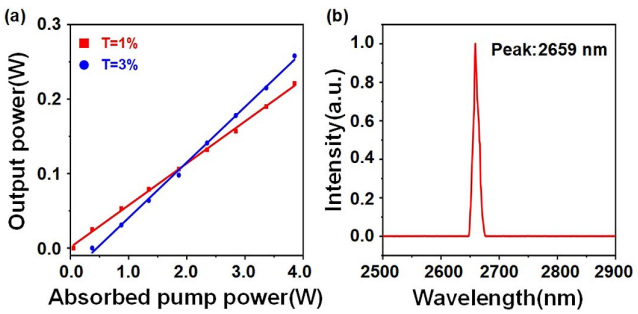

Fig. 3. (a) Laser output power versus input power with different transmissions; (b) center emission wavelength of the Er,Pr:YLF laser.

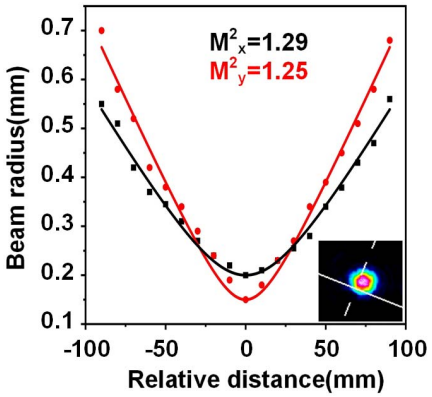

Fig. 4. Laser beam quality of the Er,Pr:YLF laser. Inset: the far-field laser beam profile.

slope efficiency of 7.4%. The laser threshold was as low as 52 mW with an OC of 1%. However, the maximum laser output power 258 mW is lower than the reported value (1.1 W) for Er:YLF, which may be caused by the fact that the shortened lifetime of the upper level $^4I_{11/2}$ is detrimental to energy storage during diode CW pumping[29]. Thus, the concentration ratio of Er^{3+} to Pr^{3+} needs to be optimized to increase the laser output power. Besides, by improving the cooling system, the compensation on the thermal effect could further enhance the output power.

The laser output spectrum was measured using an optical spectrum analyzer containing a grating spectrometer (Omni-λ 300, Zolix, China) and an InSb infrared detector (DInSb5-De01, Zolix, China), as shown in Fig. 3(b). The emission peak was located at 2659 nm, which is consistent with the measured fluorescence spectra. The output laser beam quality was analyzed by a laser beam profiler (NanoScan by Photoh, Inc). Figure 4 shows the measured laser beam quality factor M^2 and beam profile at the maximum output power. The output laser was operating in the single transverse electromagnetic TEM_{00} mode with a beam quality M^2 factor measured to be $M_x^2 = 1.29$ and $M_y^2 = 1.25$ in the horizontal and vertical directions. The output laser was measured to be linearly polarized and parallel to the *c* axis of the crystal with a polarization ratio of 9:1. The output laser stability was measured to be ±1.2% for 3 h of operation.

4. Conclusion

In conclusion, the spectroscopic and laser properties of Er,Pr:YLF crystals were studied. The absorption and fluorescence spectra were measured and analyzed by the J-O theory. The absorption cross section at 969 nm was calculated to be 0.297×10^{-20} cm^2, while the emission cross section was determined to be 1.834×10^{-20} cm^2 at 2685 nm and 1.359×10^{-20} cm^2 at 2804.6 nm, respectively. Besides, the energy transfer efficiency from $Er^{3+}:{}^4I_{13}$ to $Pr^{3+}:{}^3F_4$ was calculated to be 74.1%, indicating the effective deactivated function of the

Pr^{3+} ion. Moreover, a diode-end-pumped CW Er,Pr:YLF laser operating at 2659 nm was realized for the first time, to the best of our knowledge. A maximum output power of 258 mW is obtained with a slope efficiency of 7.4%. The higher-efficiency, higher-power Er,Pr:YLF CW lasers are expected by optimizing the concentration of Er^{3+} and Pr^{3+} ions. Our work demonstrates that the Er,Pr:YLF crystal should be a promising alternative for high-power and high-efficiency MIR laser generation.

Acknowledgement

This work was supported by the National Research Foundation of China (No. 61975095), the Young Scholars Program of Shandong University (No. 2017WLJH48), the Youth Cross Innovation Group of Shandong University (No. 2020QNQT), the Department of Science and Technology of Shandong Province (No. 2019JZZY020206), the Natural Science Foundation of Ningbo (No. 202003N4099), and the Shenzhen Science and Technology Research and Development Funds (No. JCYJ20180305163932273).

References

1. K. Scholle, S. Lamrini, P. Koopmann, and P. Fuhrberg, *2 μm Laser Sources and Their Possible Applications* (InTech, 2010).
2. A. Godard, "Infrared (2–12 μm) solid-state laser sources: a review," Comptes Rendus Physique **8**, 1100 (2007).
3. Z. L. Zhan, X. Z. Zhang, W. Q. Guo, and S. S. Xie, "Determination of ablation threshold of dental hard tissues irradiated with Er:YAG and Er,Cr:YSGG lasers," Chin. Opt. Lett. **11**, 051701 (2013).
4. I. Breunig, D. Haertle, and K. Buse, "Continuous-wave optical parametric oscillators: recent developments and prospects," Appl. Phys. B **105**, 99 (2011).
5. L. I. Isaenko and A. P. Yelisseyev, "Recent studies of nonlinear chalcogenide crystals for the mid-IR," Semicond. Sci. Technol. **31**, 123001 (2016).
6. W. T. Carnall, P. R. Fields, and K. Rajnak, "Electronic energy levels in the trivalent lanthanide aquo ions. I. Pr^{3+}, Nd^{3+}, Pm^{3+}, Sm^{3+}, Dy^{3+}, Ho^{3+}, Er^{3+}, and Tm^{3+}," J. Chem. Phys. **49**, 4424 (1968).
7. S. A. Payne, L. K. Smith, and W. F. Krupke, "Cross sections and quantum yields of the 3 μm emission for Er^{3+} and Ho^{3+} dopants in crystals," J. Appl. Phys. **77**, 4274 (1995).
8. F. H. Jagosich, L. Gomes, L. V. G. Tarelho, L. C. Courrol, and I. M. Ranieri, "Deactivation effects of the lowest excited states of Er^{3+} and Ho^{3+} introduced by Nd^{3+} ions in $LiYF_4$ crystals," J. Appl. Phys. **91**, 624 (2002).
9. H. G. Gu, Z. P. Qin, G. Q. Xie, T. Hai, P. Yuan, J. G. Ma, and L. J. Qian, "Generation of 131 fs mode-locked pulses from 2.8 μm Er:ZBLAN fiber laser," Chin. Opt. Lett. **18**, 031402 (2020).
10. S. Georgescu and O. Toma, "Er:YAG three-micron laser: performances and limits," IEEE J. Sel. Top. Quantum Electron. **11**, 682 (2005).
11. V. Lupei, S. Georgescu, and V. Florea, "On the dynamics of population inversion for 3 μm Er^{3+} lasers," IEEE J. Quantum Electron. **29**, 426 (1993).
12. S. Georgescu, O. Toma, and H. Totia, "Intrinsic limits of the efficiency of erbium 3-μm lasers," IEEE J. Quantum Electron. **39**, 722 (2003).
13. Y. Wang, Z. You, J. Li, Z. Zhu, E. Ma, and C. Tu, "Spectroscopic investigations of highly doped Er^{3+}: GGG and Er^{3+}/Pr^{3+}: GGG crystals," J. Phys. D: Appl. Phys. **42**, 215406 (2009).
14. J. Chen, D. Sun, J. Luo, H. Zhang, R. Dou, J. Xiao, Q. Zhang, and S. Yin, "Spectroscopic properties and diode end-pumped 2.79 μm laser performance of Er,Pr:GYSGG crystal," Opt. Express **21**, 23425 (2013).
15. Y. Chen, Q. Zhang, F. Peng, W. Liu, Y. He, R. Dou, H. Zhang, J. Luo, and D. Sun, "Growth, structure and radiation resistant properties of Er,Pr:GSAG laser crystals," Opt. Mater. **84**, 172 (2018).
16. Z. Fang, D. Sun, J. Luo, H. Zhang, X. Zhao, C. Quan, L. Hu, M. Cheng, Q. Zhang, and S. Yin, "Thermal analysis and laser performance of a GYSGG/Cr,Er,Pr:GYSGG composite laser crystal operated at 2.79 μm," Opt. Express **25**, 21349 (2017).
17. R. L. Aggarwal, D. J. Ripin, J. R. Ochoa, and T. Y. Fan, "Measurement of thermo-optic properties of $Y_3Al_5O_{12}$, $Lu_3Al_5O_{12}$, $YAlO_3$, $LiYF_4$, $LiLuF_4$, BaY_2F_8, $KGd(WO_4)_2$, and $KY(WO_4)_2$ laser crystals in the 80–300 K temperature range," J. Appl. Phys. **98**, 103514 (2005).
18. J. Hu, H. Xia, H. Hu, X. Zhuang, Y. Zhang, H. Jiang, and B. Chen, "Enhanced 2.7 μm emission from diode-pumped Er^{3+}/Pr^{3+} co-doped $LiYF_4$ single crystal grown by Bridgman method," Mater. Res. Bull. **48**, 2604 (2013).
19. G. S. Ofelt, "Intensities of crystal spectra of rare-earth ions," J. Chem. Phys. **37**, 511 (1962).
20. B. R. Judd, "Optical absorption intensities of rare-earth ions," Phys. Rev. **127**, 750 (1962).
21. D. K. Sardar, J. B. Gruber, B. Zandi, J. A. Hutchinson, and C. W. Trussell, "Judd–Ofelt analysis of the Er^{3+}(4f11) absorption intensities in phosphate glass: Er^{3+}, Yb^{3+}," J. Appl. Phys. **93**, 2041 (2003).
22. X.-Y. Yu, H.-B. Chen, S.-J. Wang, Y.-F. Zhou, A.-H. Wu, and S.-X. Dai, "Growth and spectral properties of Er^{3+}:$LiYF_4$ single crystal," J. Inorg. Mater. **26**, 923 (2011).
23. D. K. Sardar, S. Chandrasekharan, K. L. Nash, and J. B. Gruber, "Optical intensity analyses of Er^{3+}:$YAlO_3$," J. Appl. Phys. **104**, 023102 (2008).
24. G. A. Kumar, R. Riman, S. C. Chae, and Y. N. Jang, "Synthesis and spectroscopic characterization of CaF_2:Er^{3+} single crystal for highly efficient 1.53 μm amplification," J. Appl. Phys. **95**, 3243 (2004).
25. Y. Tian, R. Xu, L. Hu, and J. Zhang, "Spectroscopic properties and energy transfer process in Er^{3+} doped ZrF_4-based fluoride glass for 2.7 μm laser materials," Opt. Mater. **34**, 308 (2011).
26. P. A. Loiko, E. A. Arbabzadah, M. J. Damzen, X. Mateos, E. B. Dunina, A. A. Kornienko, A. S. Yasukevich, N. A. Skoptsov, and K. V. Yumashev, "Judd–Ofelt analysis and stimulated-emission cross-sections for highly doped (38 at.%) Er:YSGG laser crystal," J. Lumin. **171**, 226 (2016).
27. M. Tikerpae, S. D. Jackson, and T. A. King, "Theoretical comparison of Er^{3+}-doped crystal lasers," J. Modern Opt. **45**, 1269 (1998).
28. J. Koetke and G. Huber, "Infrared excited-state absorption and stimulated-emission cross sections of Er^{3+}-doped crystals," Appl. Phys. B **61**, 151 (1995).
29. T. Jensen, A. Diening, G. Huber, and B. H. T. Chai, "Investigation of diode-pumped 2.8-μm Er:$LiYF_4$ lasers with various doping levels," Opt. Lett. **21**, 585 (1996).